rather than an increased susceptibility given the overlap between ILD and COVID-19 symptoms. This confounding, however, would tend to bias our data toward the null by capturing patients with less severe disease. 4) Constrained geographic area potentially limits the generalizability of our conclusions. Ongoing larger international studies will help further elucidate the risk factors and outcomes of patients with ILD and COVID-19.

In summary, in this multicenter case–control study, patients with ILD, particularly those of advanced age, had increased odds of severe disease and death from COVID-19. Patients with ILD should be counseled of their increased risk, with an emphasis on public health measures to prevent infection in this susceptible population. ∎

Author disclosures are available with the text of this letter at www.atsjournals.org.

Anthony J. Esposito, M.D.*
Aravind A. Menon, M.D.*
Auyon J. Ghosh, M.D.*
Rachel K. Putman, M.D., M.P.H.
Laura E. Fredenburgh, M.D., C.M.
Souheil Y. El-Chemaly, M.D., M.P.H.
Hilary J. Goldberg, M.D., M.P.H.
Rebecca M. Baron, M.D.
Gary M. Hunninghake, M.D., M.P.H.
Tracy J. Doyle, M.D., M.P.H.‡
Brigham and Women's Hospital
Boston, Massachusetts

ORCID IDs: 0000-0002-8636-0845 (A.J.E.); 0000-0002-0211-4509 (A.A.M.); 0000-0003-0334-4039 (A.J.G.); 0000-0002-8027-7450 (R.K.P.); 0000-0002-7447-6453 (L.E.F.); 0000-0003-2929-5589 (S.Y.E.-C.); 0000-0002-2319-0009 (H.J.G.); 0000-0003-1673-9523 (R.M.B.); 0000-0001-9782-2841 (G.M.H.); 0000-0002-0770-1059 (T.J.D.).

*These authors contributed equally to this work.
‡Corresponding author (e-mail: tjdoyle@bwh.harvard.edu).

References

1. Guan WJ, Liang WH, Zhao Y, Liang HR, Chen ZS, Li YM, et al.; China Medical Treatment Expert Group for COVID-19. Comorbidity and its impact on 1590 patients with COVID-19 in China: a nationwide analysis. Eur Respir J 2020;55:2000547.
2. Yang J, Zheng Y, Gou X, Pu K, Chen Z, Guo Q, et al. Prevalence of comorbidities and its effects in patients infected with SARS-CoV-2: a systematic review and meta-analysis. Int J Infect Dis 2020;94: 91–95.
3. Alqahtani JS, Oyelade T, Aldhahir AM, Alghamdi SM, Almehmadi M, Alqahtani AS, et al. Prevalence, severity and mortality associated with COPD and smoking in patients with COVID-19: a rapid systematic review and meta-analysis. PLoS One 2020;15:e0233147.
4. Li X, Xu S, Yu M, Wang K, Tao Y, Zhou Y, et al. Risk factors for severity and mortality in adult COVID-19 inpatients in Wuhan. J Allergy Clin Immunol 2020;146:110–118.
5. Fu L, Wang B, Yuan T, Chen X, Ao Y, Fitzpatrick T, et al. Clinical characteristics of coronavirus disease 2019 (COVID-19) in China: a systematic review and meta-analysis. J Infect 2020;80:656–665.
6. Garg S, Kim L, Whitaker M, O'Halloran A, Cummings C, Holstein R, et al. Hospitalization rates and characteristics of patients hospitalized with laboratory-confirmed coronavirus disease 2019 - COVID-NET, 14 states, March 1-30, 2020. MMWR Morb Mortal Wkly Rep 2020;69: 458–464.
7. Southern BD. Patients with interstitial lung disease and pulmonary sarcoidosis are at high risk for severe illness related to COVID-19. Cleve Clin J Med [online ahead of print] 18 Jun 2020; DOI: 10.3949/ccjm.87a.ccc026.
8. Azadeh N, Limper AH, Carmona EM, Ryu JH. The role of infection in interstitial lung diseases: a review. Chest 2017;152:842–852.
9. Horby P, Lim WS, Emberson JR, Mafham M, Bell JL, Linsell L, et al.; RECOVERY Collaborative Group. Dexamethasone in hospitalized patients with COVID-19 - preliminary report. N Engl J Med [online ahead of print] 17 Jul 2020; DOI: 10.1056/NEJMoa2021436.
10. Li H, Chen C, Hu F, Wang J, Zhao Q, Gale RP, et al. Impact of corticosteroid therapy on outcomes of persons with SARS-CoV-2, SARS-CoV, or MERS-CoV infection: a systematic review and meta-analysis. Leukemia 2020;34:1503–1511.

Check for updates
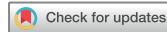
Effect of Positive End-Expiratory Pressure and Proning on Ventilation and Perfusion in COVID-19 Acute Respiratory Distress Syndrome

To the Editor:

Assessment of lung ventilation and perfusion of coronavirus disease (COVID-19) with acute respiratory distress syndrome (C-ARDS) is still scarce, especially in response to positive end-expiratory pressure (PEEP) and prone positioning. The objective of this study was to describe the physiological effects of PEEP and prone position on respiratory mechanics, ventilation, and pulmonary perfusion in patients with C-ARDS.

Methods

ARDS was defined according to the Berlin definition (1), and severe acute respiratory syndrome coronavirus 2 (SARS-CoV-2) infection was confirmed by positive nasopharyngeal PCR. Patients were included consecutively, within 72 hours of intubation, if the electrical impedance tomography (EIT) device was available. Patients with a contraindication to esophageal catheter (esophageal stenosis, varices, or ulceration in particular) and/or impedancemetry (pacemaker, implantable defibrillator, or skin lesion) were excluded. Patients were deeply sedated and paralyzed. An EIT (Enlight 1800; Timpel) assessed regional ventilation and perfusion. Lung perfusion was recorded during an expiratory pause by injecting a 10-ml bolus of 7.5% hypertonic saline solution into a central venous catheter. Respiratory mechanics, ventilation, and perfusion EIT data were recorded at three arbitrary levels of PEEP (18, 12, and 6 cm H_2O) in the supine position and at PEEP 12 cm H_2O after 3 (2–4) hours of prone position. Arterial blood gases were collected prior

Table 1. Clinical Data, Respiratory Mechanics, Ventilation, and Perfusion in Supine Position (at Three Levels of PEEP) and Prone Position in Patients with COVID-19 with Acute Respiratory Distress Syndrome

	Supine				Prone	
	PEEP 6 cm H$_2$O	PEEP 12 cm H$_2$O	PEEP 18 cm H$_2$O	P Friedman	PEEP 12 cm H$_2$O	P Wilcoxon
Ventilator settings						
F$_{IO_2}$, %	70 (70 to 80)	70 (70 to 80)	70 (70 to 80)	>0.99	70 (60 to 80)	0.94
End-tidal volume, ml	400 (400 to 420)	400 (400 to 420)	400 (400 to 420)	>0.99	400 (400 to 400)	>0.99
Respiratory rate, cycles/min	28 (28 to 33)	28 (28 to 33)	28 (28 to 33)	>0.99	32 (28 to 24)	0.37
Respiratory mechanics						
Pplat, cm H$_2$O	17 (16 to 18)	22 (21 to 24)*	33 (29 to 33)*†	<0.01	23 (21 to 25)	0.31
PEEPtot, cm H$_2$O	7 (7 to 8)	13 (13 to 13)*	19 (18 to 19)*†	<0.01	14 (13 to 14)	0.09
ΔP, cm H$_2$O	9 (8 to 11)	9 (8 to 10)	14 (10 to 15)	<0.01	10 (7 to 12)	0.34
PLend-insp, cm H$_2$O	14 (12 to 14)	15 (14 to 19)*	24 (23 to 26)*†	<0.01	14 (12 to 21)	0.59
PLend-exp, cm H$_2$O	0 (−4 to 1)	2 (1 to 5)*	5 (4 to 7)*†	<0.01	3 (2 to 5)	0.40
ΔPL, cm H$_2$O	7 (6 to 8)	6 (5 to 9)	11 (8 to 11)	<0.01	6 (4 to 10)	0.93
CRS, ml/cm H$_2$O	44 (36 to 51)	44 (38 to 55)	29 (25 to 43)	<0.01	39 (32 to 53)	0.19
CCW, ml/cm H$_2$O	191 (147 to 294)	162 (147 to 192)	162 (98 to 191)	0.01	123 (103 to 140)	0.12
CL, ml/cm H$_2$O	58 (42 to 64)	64 (45 to 77)	38 (34 to 54)	<0.01	66 (41 to 93)	0.43
Stress index >1	0/9 (0%)	1/9 (11%)	7/9 (75%)*†	<0.01	2/9 (22%)	>0.99
Clinical data						
CO, L/min	8.2 (6.8 to 9.8)	7.6 (5.9 to 8.5)*	7.1 (4.9 to 7.6)*	<0.01	7.5 (6.4 to 8.1)	0.89
Sp$_{O_2}$, %	93 (92 to 96)	96 (93 to 98)	98 (93 to 99)	0.02	96 (95 to 97)	0.72
P$_{ETCO_2}$, mm Hg	34 (30 to 35)	35 (32 to 37)	34 (31 to 37)	0.04	34 (33 to 38)	0.26

Definition of abbreviations: Ccw = chest wall compliance [Ccw = VT/(Pes-insp − Pes-exp)]; CL = lung compliance (CL = VT/[(Pplat − Pes-insp) − (PEEPtot − Pes-exp)]); CO = cardiac output; COVID-19 = coronavirus disease; Crs = respiratory system compliance [Crs = VT/(Pplat − PEEPtot)]; ΔP = driving pressure (ΔP = Pplat − PEEPtot); ΔPL = transpulmonary driving pressure [ΔPL = (Pplat − Pes-insp) − (PEEPtot − Pes-exp)]; EL = lung elastance; ERS = respiratory system elastance; PEEP = positive end-expiratory pressure; PEEPtot = total PEEP; Pes-exp = end-expiratory esophageal pressure; Pes-insp = end-inspiratory esophageal pressure; P$_{ETCO_2}$ = end-tidal carbon dioxide pressure; PLend-exp = end-expiratory transpulmonary pressure (PLend-exp = PEEPtot − Pes-exp); PLend-insp = elastance ratio–derived end-inspiratory transpulmonary pressure [PLend-insp = (EL × Pplat)/ERS]; Pplat = plateau pressure; Sp$_{O_2}$ = oxygen saturation as measured by pulse oximetry.
$N = 9$. Continuous variables are expressed as median (first quartile to third quartile). For quantitative variables, paired Wilcoxon test with Benjamini-Hochberg correction, after a significant Friedman test, was used to determine significance; for qualitative variables, McNemar or exact Fisher's test with Benjamini-Hochberg correction, after a significant Cochrane Q test was used.
*$P < 0.05$ compared with PEEP 6 cm H$_2$O.
†$P < 0.05$ compared with PEEP 12 cm H$_2$O.

to exploration, prior to prone positioning, and at the end of proning. The following parameters were collected in each phase: expiratory VT, peak pressure, plateau pressure, total PEEP, end-inspiratory and end-expiratory esophageal pressure (Nutrivent; Sidam), pulse oximetry, end-tidal expired carbon dioxide pressure, respiratory rate, heart rate, blood pressure, and cardiac output (CO, FloTrac system; Edwards Lifesciences).

EIT data analysis. We separated the lung into a dependent area corresponding to the posterior half (dorsal) and a nondependent area corresponding to the anterior half (ventral) of the lung EIT image taken in supine position. We measured the following parameters in dependent and nondependent lung regions: impedance variation during ventilation (ΔZv̇) and perfusion (ΔZQ̇) and relative distribution of ventilation and perfusion, VT distending lung regions, regional respiratory system compliance (2), and V̇A/Q̇ ratio for each pixel derived from the formula, assuming a 30% fixed anatomical dead space:

$$\frac{\dot{V}_A(pixel)}{\dot{Q}(pixel)} = \frac{\frac{\Delta Z\dot{v}(pixel)}{\Delta Z\dot{v}(total)} \times (V_T \times \text{respiratory rate} \times 0.7)}{\frac{\Delta Z\dot{Q}(pixel)}{\Delta Z\dot{Q}(total)} \times CO}.$$

The V̇A/Q̇ ratio of each pixel was used to define shunt (severe if <0.1 and moderate if between 0.1 and 0.5) or a dead space (severe if >10 and moderate if between 2 and 10). The shunt fraction was the fraction of CO perfusing the shunt pixels. The dead space fraction was the fraction of alveolar ventilation supplying the dead space pixels.

This is an ancillary report of two ongoing prospective observational studies on ARDS (CPP-66/17 and IRB-2018-A00867-48).

Statistics. Quantitative data are expressed as median (first to third quartile). Effects of PEEP were analyzed by Friedman test followed by Wilcoxon paired test with Benjamini-Hochberg correction for multiple testing. Effects of prone positioning were studied using Wilcoxon paired test.

Results
Among 41 patients with C-ARDS admitted during the study period, 9 completed full explorations and could be analyzed (8 male; age, 53 [50–60] yr; body mass index, 33.1 [29.8–35.6] kg/m²; Pa$_{O_2}$/FI$_{O_2}$, 133 [96–140] mm Hg). Effects of PEEP titration and prone position are summarized in Table 1 and Figure 1 (including an illustrative typical response).

PEEP. Ventilation was predominantly ventral at low PEEP and dorsal at high PEEP, and the anteroposterior gradient got inversed with the increase in PEEP. This inversion was mainly driven by ventral hyperdistention (as suggested by the decrease in ventral
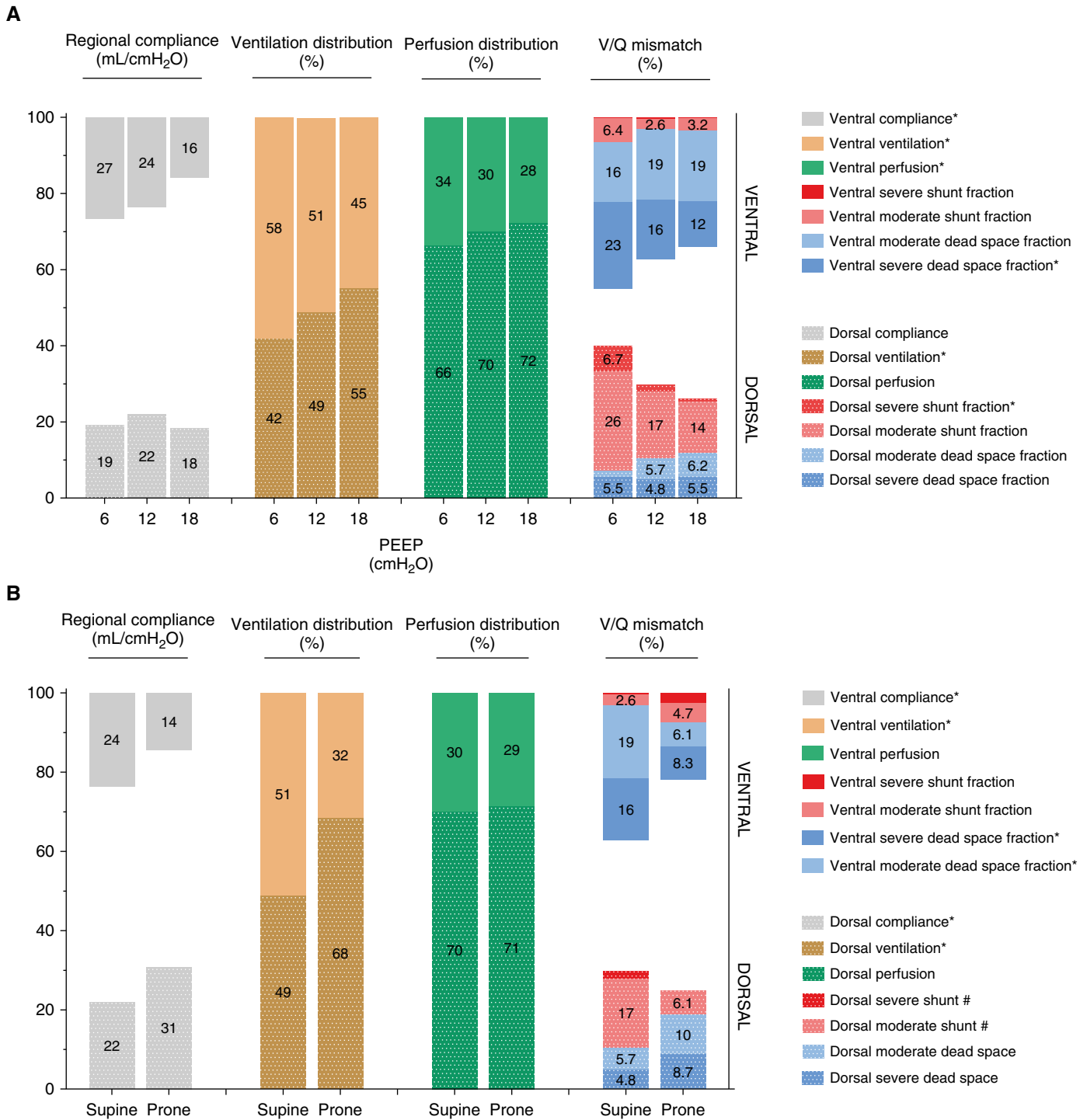
Figure 1. (*A–C*) Respiratory system compliance, ventilation, and perfusion distribution in supine position at three levels of positive end-expiratory pressures (PEEPs) (*A*) and in prone position (*B*) in nine patients with coronavirus disease acute respiratory distress syndrome with an illustrative case showing a typical response (*C*). For better illustration, data are shown as mean (not median) values. *$P < 0.05$ and #$P < 0.06$ for the comparison of tested conditions. For the illustrative case in the supine position, the ventral parts of the lungs are upstream and the dorsal parts are downstream, and vice versa in the prone position. On the color scale, lung areas with a $\dot{V}_A/\dot{Q}$ ratio near 1 are green, whereas those with lower values tend to be red/dark and those with higher values are blue. The red areas are more prominent in supine position, especially at low PEEP, but less at high PEEP and always in dorsal regions. The blue areas are also more prominent in supine and always in ventral regions.
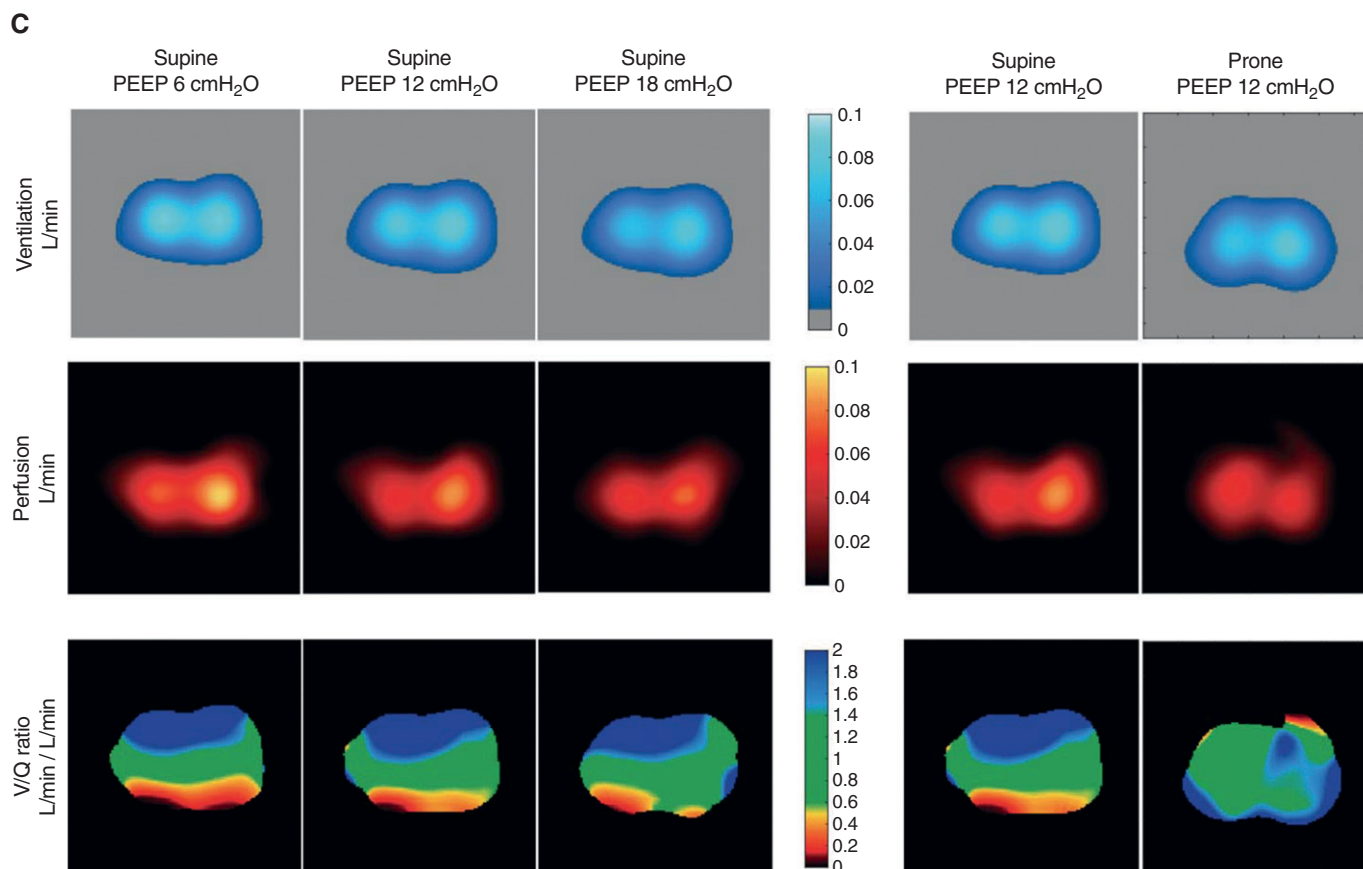
C

Figure 1. (*Continued*).

compliance and the increase in driving pressure, end-inspiratory transpulmonary pressure, and stress index at higher PEEP). Lung perfusion was predominant in the dorsal areas regardless of the PEEP level, but the increase in PEEP reduced CO and further decreased absolute ventral perfusion. Increased PEEP also reduced the proportion of ventral severe dead space and dorsal severe shunt.

Prone position. Turning the patient from supine to prone position increased $Pa_{O_2}/F_{I_{O_2}}$ ratio by 64 mm Hg (41–90) and induced recruitment in dorsal regions (i.e., increase in dorsal regional compliance) and collapse in ventral regions (i.e., decrease in ventral regional compliance), but it did not change the dorsal predominance of pulmonary perfusion. Proning decreased ventral dead space and dorsal shunt. The decrease in chest wall compliance was not significant, and lung compliance was not affected.

Discussion

The effects of PEEP in C-ARDS were close to those reported in classical ARDS. The increase in PEEP resulted in alveolar recruitment associated with a significant decrease in severe shunt, mainly in the dorsal regions, driven by the increase in dorsal ventilation. Additionally, increasing PEEP resulted in less severe alveolar dead space in the ventral regions because ventilation decreased more than perfusion. However, the better $\dot{V}_A/\dot{Q}$ matching at high PEEP was at the price of a clear

hyperdistention as suggested by the respiratory mechanics data and, in particular, by the decrease in ventral compliance and ventilation.

The effect of prone position was also comparable to that previously observed in classical ARDS. Typically, proning provokes recruitment of dorsal areas and collapse of ventral areas (3), does not change predominantly dorsal pulmonary perfusion in experimental studies (4), and eventually improves $\dot{V}_A/\dot{Q}$ ratios (4) and, consequently, oxygenation, all of which we proved for the first time in our human study. On the one hand, prone position decreases the dorsal shunt because it increases ventilation in this zone and maintains its rich perfusion. On the other hand, proning decreases the ventral dead space because it decreases ventilation in a zone that is poorly perfused. Overall, there was no improvement in lung compliance, which is variable in prone position (5, 6) and depends on the ratio between dorsal recruitment and ventral collapse. The decrease in chest wall compliance did not reach significance, probably because of the small sample size.

The dead space fraction seemed to exceed the shunt fraction in the various tested situations. On the same line, previous work suggested that $\dot{V}_A/\dot{Q}$ mismatch resulted from having ventilated but nonperfused areas in C-ARDS (7). Many reports have highlighted severe pulmonary vascular dysfunction in C-ARDS with high rates of pulmonary embolism and *in situ* thrombosis (8).

The main limitations include the small sample size, highly selected cohort, single PEEP level in prone position, lack of repeated blood gases with PEEP titration (because of specific safety measures at the beginning of the COVID-19 pandemic), and estimation of a fixed anatomical dead space. These preliminary results should be confirmed in a larger population.

Conclusions. Prone positioning and, to a lesser extent, increased PEEP shifted ventilation from ventral to dorsal regions in patients with C-ARDS but did not change perfusion, which remained predominantly dorsal, resulting in better $\dot{V}_A/\dot{Q}$ matching. ∎

Author disclosures are available with the text of this letter at www.atsjournals.org.

François Perier, M.D.*‡
Samuel Tuffet, M.D.*
Assistance Publique-Hôpitaux de Paris,
Centre Hospitalier Universitaire Henri Mondor
Créteil, France
and
Université Paris Est-Créteil
Créteil, France

Tommaso Maraffi, M.D.
Assistance Publique-Hôpitaux de Paris,
Centre Hospitalier Universitaire Henri Mondor
Créteil, France
and
Centre Hospitalier Intercommunal de Créteil
Créteil, France

Glasiele Alcala, M.D.
Marcus Victor, Ph.D.
University of São Paulo
São Paulo, Brazil

Anne-Fleur Haudebourg, M.D.
Nicolas De Prost, M.D., Ph.D.
Assistance Publique-Hôpitaux de Paris,
Centre Hospitalier Universitaire Henri Mondor
Créteil, France
and
Université Paris Est-Créteil
Créteil, France

Marcelo Amato, M.D., Ph.D.
University of São Paulo
São Paulo, Brazil

Guillaume Carteaux, M.D., Ph.D.
Armand Mekontso Dessap, M.D., Ph.D.
Assistance Publique-Hôpitaux de Paris,
Centre Hospitalier Universitaire Henri Mondor
Créteil, France
and
Université Paris Est-Créteil
Créteil, France

ORCID ID: 0000-0002-4833-4320 (N.D.P.).

*These authors contributed equally to this work.
‡Corresponding author (e-mail: francois.perier@aphp.fr).

References

1. Ranieri VM, Rubenfeld GD, Thompson BT, Ferguson ND, Caldwell E, Fan E, *et al*.; ARDS Definition Task Force. Acute respiratory distress syndrome: the Berlin Definition. *JAMA* 2012;307: 2526–2533.
2. Mauri T, Eronia N, Turrini C, Battistini M, Grasselli G, Rona R, *et al*. Bedside assessment of the effects of positive end-expiratory pressure on lung inflation and recruitment by the helium dilution technique and electrical impedance tomography. *Intensive Care Med* 2016;42: 1576–1587.
3. Gattinoni L, Pelosi P, Vitale G, Pesenti A, D'Andrea L, Mascheroni D. Body position changes redistribute lung computed-tomographic density in patients with acute respiratory failure. *Anesthesiology* 1991; 74:15–23.
4. Richter T, Bellani G, Scott Harris R, Vidal Melo MF, Winkler T, Venegas JG, *et al*. Effect of prone position on regional shunt, aeration, and perfusion in experimental acute lung injury. *Am J Respir Crit Care Med* 2005;172:480–487.
5. Pelosi P, Tubiolo D, Mascheroni D, Vicardi P, Crotti S, Valenza F, *et al*. Effects of the prone position on respiratory mechanics and gas exchange during acute lung injury. *Am J Respir Crit Care Med* 1998;157:387–393.
6. Riad Z, Mezidi M, Subtil F, Louis B, Guérin C. Short-term effects of the prone positioning Maneuver on lung and chest wall mechanics in patients with acute respiratory distress syndrome. *Am J Respir Crit Care Med* 2018;197:1355–1358.
7. Mauri T, Spinelli E, Scotti E, Colussi G, Basile MC, Crotti S, *et al*. Potential for lung recruitment and ventilation-perfusion mismatch in patients with the acute respiratory distress syndrome from coronavirus disease 2019. *Crit Care Med* 2020;48: 1129–1134.
8. Ackermann M, Verleden SE, Kuehnel M, Haverich A, Welte T, Laenger F, *et al*. Pulmonary vascular endothelialitis, thrombosis, and angiogenesis in Covid-19. *N Engl J Med* 2020;383: 120–128.

Check for updates

Association of Mortality with Neuromuscular Blockade Differs according to Baseline Diaphragm Thickness

To the Editor:

Spontaneous breathing during mechanical ventilation may lead to worsening lung injury in acute respiratory distress syndrome (ARDS), particularly when high inspiratory efforts that limit the application of lung-protective ventilation are present (1). This hypothesized mechanism of lung injury has been referred to as patient self-inflicted lung injury (P-SILI). High regional transpulmonary pressures secondary to vigorous inspiratory efforts can increase regional lung *stress* and *strain*, resulting in local volutrauma (2). Because the intensity of these inspiratory efforts will depend, at least in part, on the force-generating capacity of the diaphragm, patients with greater diaphragm muscle mass and strength may be at higher risk. This hypothesis is indirectly supported by the recent description of asymmetrically distributed fibrosis in two patients with idiopathic pulmonary fibrosis and hemidiaphragm weakness and atrophy: computed tomography scanning revealed that lesions were restricted to the hemithorax